ACS Sustainable Chemistry & Engineering

Research Article

pubs.acs.org/journal/ascecg

General and Green Strategy toward High Performance Positive Electrode Materials for Rechargeable Li Ion Batteries with Crop Stalks as the Host Carbon Matrixes

Haitao Xu, Huijuan Zhang, Yanping Mu, Yangyang Feng, and Yu Wang*

The State Key Laboratory of Mechanical Transmissions and the School of Chemistry and Chemical Engineering, Chongqing University, 174 Shazheng Street, Shapingba District, Chongqing City 400044, People's Republic of China

Supporting Information

ABSTRACT: A novel, simple and universal approach toward the sheetlike carbon composites is presented here. In the method, an abundant agricultural byproduct (produced at a rate of 2.2×10^7 tons/year in China), obtained from the sustainable, environmentally friendly crop stalks, was used as a porous template for large-scale production of high performance cathode materials for lithium ion batteries. Owing to the large surface area, porous structure and small size of the functional particles, the nanocomposites manifest excellent electrochemical performance. Furthermore, the porous structure and charge transport property of the carbon materials can provide an electronic conductive network and promote the lithium ion extraction/insertion. In particular, the prepared $LiFePO_4/C$ composites present a high reversible capacity of 158 mAh g^{-1} after 500 cycles, indicating crop stalks can be a massive resource for high performance lithium ion batteries.

KEYWORDS: *Crop stalks, Biomass, Carbon composites, Lithium ion batteries, Electrode materials*

INTRODUCTION

Corn, first domesticated and cultivated in the Americas long before Europeans reached the New World, is the most produced crop species worldwide.[1] It has long been one of the greatest botanical riddles across the globe (8.504×10^8 metric tons/year).[2] However, the annual biomass wastes exceed 0.7 billion tons in China, among which the cornstalk, wheat straw and straw wastes are around 220, 110 and 180 million tons per year, respectively.[3] In addition, the current applications of the crop stalks have been very limited to the lowly added-value fields, such as fodder, fertilizer, producing furniture or fuel.[4] Moreover, the huge amount of byproduct is an environmental nuisance, especially when the peasants burn crop stalks.[3,5] So, there is an increasing demand for developing more valuable applications of the "waste" resources.

The major ingredients of crop stalks, cellulose, hemicellulose and lignin, turn into porous carbon materials after being calcined in an inert atmosphere.[6] As far as we can see, porous carbon materials have regular pores, large specific surface area, good thermal stability and chemical stability,[7−9] which endow them with a tremendous series of potential applications in many important fields, for example, adsorption,[10] catalysis,[11] hydrogen storage[12] and Li ion batteries.[13] As is known to all, with the speeding development of the economic society, the energy demand is rapidly increasing. However, sharp reduction of finite reserved fossil fuel and environmental pollution brought by fossil fuel's exhaustion are calling for more alternative energy sources. Lithium ion batteries (LIBs) have already proved themselves the most advanced electrochemical energy storage systems for a wide range of applications, including portable electronics, hybrid electric vehicles and large industrial equipment.[14,15]

Recently, many works based on natural biomass sources and green materials were carried out. Our group employed low-cost and environmentally friendly glucose as the carbon source to fabricate sandwiched graphene sheets and peapodlike carbon composites, which were ideal materials for energy storage.[16,17] Jung et al.[18] took advantage of the interconnected nanoporous structure naturally existing in rice husks and finally obtained 3D porous Si as a high performance Li ion battery anode, where the Si anode reversibly delivered a capacity of 1615 mAh g^{-1} at 0.1 C. Meng et al.[19] adopted a silk cocoon to prepare hierarchically porous carbon materials in encapsulating sulfur composites, which achieved a specific capacity of around 1443 mAh g^{-1} at 0.1 C. Chen et al.[20] adopted rice straws to prepare high surface area and hierarchical porous carbon materials, and the obtained carbon materials showed large reversible capacity at high charge/discharge rates. In conclusion, many works use

Received: April 24, 2015
Revised: June 7, 2015
Published: June 9, 2015

DOI: 10.1021/acssuschemeng.5b00350
ACS Sustainable Chem. Eng. 2015, 3, 1650−1657

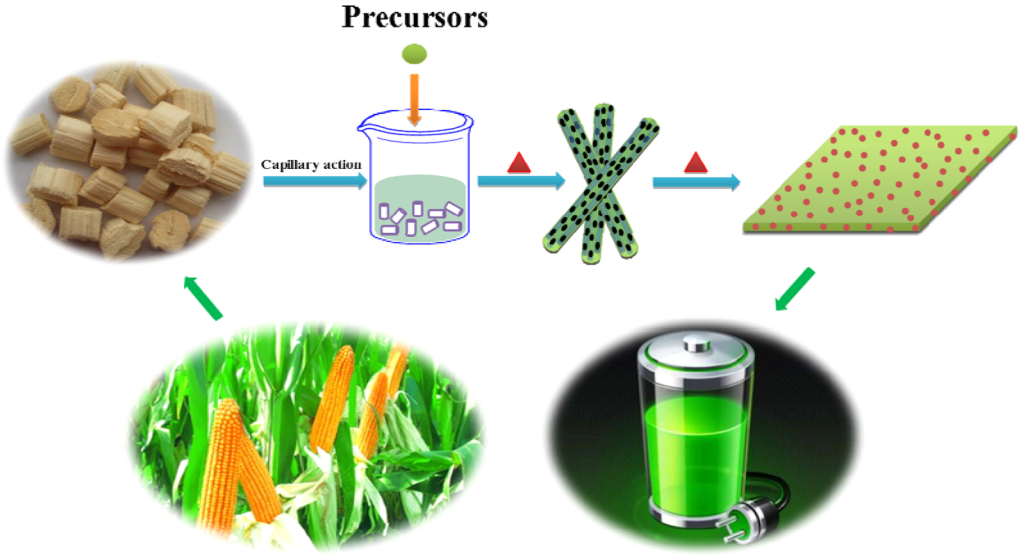

Figure 1. Schematic illustration to introduce the general fabrication route toward the sheetlike carbon composites.

biofeed stock to prepare Si/C,[18,20,21] MnO_2/C,[22] porous carbon[23] and S/C composite.[19] However, it is almost the first time for us to introduce a general strategy to prepare nanostructured carbon composites for high performance LIBs. As illustrated in our paper, we have successfully fabricated both cathode and anode materials for LIBs, for instance, $LiFePO_4$, Li_2FeSiO_4 and Sn. In contrast, to the best of our knowledge, there is almost no report on cathode materials derived from biofeed stock for LIBs.[18,21−25] Notably, we have made a major breakthrough in this work, in which the general fabrication strategy based on biofeed stock expands its scope of application from a simple substance or metal oxide to a ternary compound.[18,21−29]

Herein, we report a novel and general strategy to apply crop stalks into the synthesis of carbon composites for high performance Li ion batteries, in which the crop stalks are used as host carbon matrixes for nanoparticles. As shown in the flowchart in Figure 1, precursor solutions are first sucked into the pores of raw crop stalks under the aid of capillary action, followed by calcinations in an inert atmosphere. Finally, we obtain sheetlike porous carbon composites, in which functional materials are embedded in the porous carbon matrixes. Compared with other materials derived from natural biopolymeric and traditional synthetic method for Li ion batteries, our strategy has several advantages: (I) In contrast with other biological materials, corn, as the environmentally friendly and low-cost source, possesses superiority to reduce make product cost. (II) A simple and energy-efficient method is outstanding among the conventional approaches toward the synthesis of electrode materials for LIBs. Besides, byproduct in the fabrication has not been observed, which is in accordance with the requirements of the green society. (III) The successful syntheses of both cathode and anode materials for LIBs, for instance, $LiFePO_4$, Li_2FeSiO_4, $LiMnPO_4$ and Sn (Figure S6 of the Supporting Information), prove that it is a general fabrication strategy. (IV) The naturally nanoporous carbon matrix stemming from crop stalks not only prevents the nanoparticles from aggregation but also serves as an electrolyte diffusing channels for high-rate operation, as well as an elastic buffer to relieve the mechanical strain during Li^+ insertion/extraction. Moreover, the sheetlike carbon composites possess excellent conductivity, which can significantly accelerate the charge transfer rate. (V) The prepared porous carbon composites are pure-phase, and active materials' particles dotted in the carbon network are within tens of nanometers, resulting in the short Li^+ intercalation distance. In general, the facile fabrication strategy is beneficial to generating high performance electrode materials for Li ion batteries, which have a highly reversible specific capacity, good rate ability and remarkable cyclability.

RESULTS AND DISCUSSION

The crop stalks used in the current study were harvested from the farmland of Shandong province in China. Figure 1 illustrates the general fabrication strategy. As shown in the digital photograph, the raw crop stalks have a loose and porous structure, possessing enormously absorbent ability for precursor solutions due to the capillary action. As shown in Figure S7a of the Supporting Information, the crop stalks are made up with sheetlike carbon sheets, dominated by layer-by-layer stacking. Besides, there are amounts of void space between carbon sheets verified by cross section SEM imaging in Figure S7b of the Supporting Information. Then the fully soaked crop stalks are dried in the oven, and as a result, moisture is removed from the pores. Afterward, the intermediate products are calcined in a tube furnace. The major ingredients of crop stalks (cellulose, hemicellulose and lignin) were oxidized to sheetlike carbon and accompanying evolution of H_2O, P, CO or CO_2 definitely results in a porous structure across the surface of the carbon sheets. The morphology of final product is nanosheet encapsulated with functional nanoparticles. As we can see from the schematic illustration, the nanoparticles are embedded into the porous carbon matrixes, providing a convenient environment for insertion and extraction of Li^+.[30] The applied fabrication strategy here supplies a unique and low-cost method to yield nanoporous carbon/active materials composites on a large scale, which will potentially deliver high reversible capacity, good cyclability and rate capability.

Figure 2a shows the X-ray diffraction (XRD) patterns of $LiFePO_4$/C nanocomposite calcinated at different temperatures, in which all the diffraction lines can be indexed to the orthorhombic $LiFePO_4$ phase (JCPDS Card No. 40-1499).

DOI: 10.1021/acssuschemeng.5b00350
ACS Sustainable Chem. Eng. 2015, 3, 1650−1657

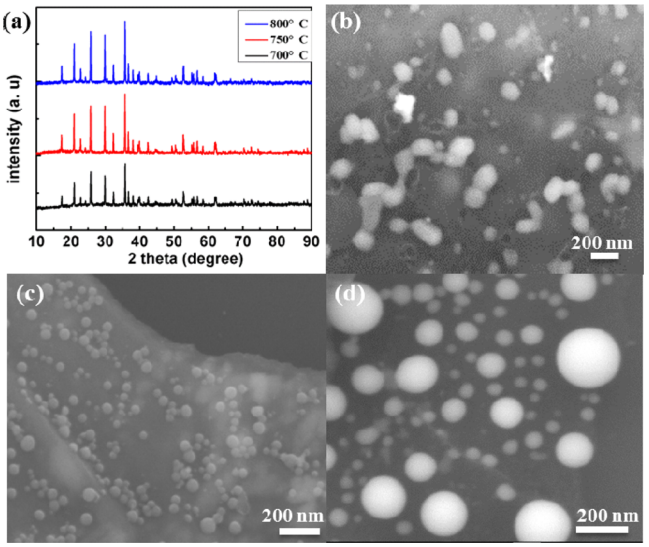

Figure 2. (a) XRD patterns of $LiFePO_4/C$ nanocomposite calcinated at different temperatures. (b, c, d) SEM images of $LiFePO_4/C$ calcinated at 700, 750 and 800 °C.

Normally, the extensive synthesis temperature for the $LiFePO_4/C$ nanocomposite is a crucial parameter for industrial production. It is obvious to find that the XRD intensity increases along with the calcination temperature, implying that the crystallization of $LiFePO_4$ is better at higher temperatures.[31] As verified in Figure 2b,c,d, the scanning electron microscopy (SEM) images, higher synthesis temperature results in undesirable growth of particles and collapsing of nanostructures.[32,33] However, higher temperature is in favor of improving crystal integrity and then enhancing electronic conductivity, which is one of the key factors to strengthen electrochemical performance. Hence, a balanced temperature should be sought for and 750 °C is such a balance temperature between minimizing particle's size and maintaining good enough crystallization and electronic conductivity. Besides, no broad peak as a sign of amorphous carbon can be identified from the XRD pattern, indicating that the carbon matrixes maybe are crystallized. This has been further confirmed and evidenced by the appearance of a strong G peak in the Raman spectrum of the $LiFePO_4/C$ nanocomposite (Figure S1 of the Supporting Information). The Raman spectrum of the nanocomposite exhibits two peaks at 1580 cm^{-1} (G band) and 1360 cm^{-1} (D band), corresponding to the vibrations of carbon atoms with sp^2 electronic configuration, and the disordered and imperfect structures of carbon materials, respectively.[34] In addition, the intensity of the G band is nearly the same as that of the D band, implying the good crystallinity of carbon. Nitrogen isothermal adsorption–desorption measurements were performed to determine the porous structure and Brunauer–Emmett–Teller (BET) surface areas of the $LiFePO_4/C$ nanocomposite. According to BET analysis in Figure 3, a total specific surface area of 483.66 m^2 g^{-1} is obtained. The Barrett–Joyner–Halenda (BJH) pore-size distribution, shown in the inset of Figure 3, indicates that the mesopores of carbon matrix mainly focus at 3.8 and 7 nm, respectively. The large surface area and mesopores make it possible for carbon matrixes and active materials' being fully infiltrated into the electrolyte, which is greatly beneficial for Li^+ rapidly shuttling between electrolyte and $LiFePO_4/C$ composite.[35] To test the carbon content precisely, ICP-AES was conducted and the result was 7.09%.

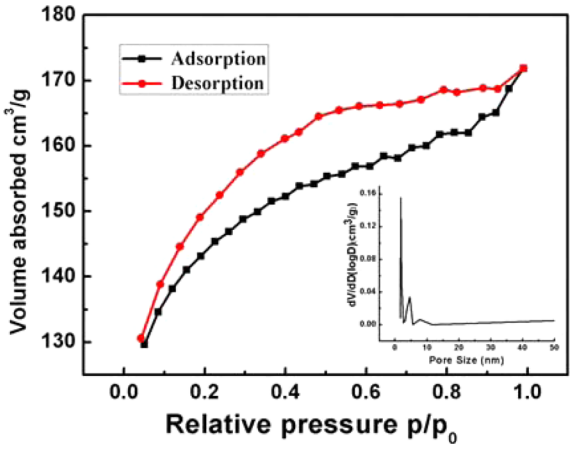

Figure 3. N_2 adsorption–desorption isotherms of $LiFePO_4/C$ at 750 °C. The inset shows the respective pore size distributions.

The morphology and microstructure of the as-prepared mesoporous $LiFePO_4/C$ nanocomposite are analyzed by field emission scanning electron microscopy (FESEM), transmission electron microscopy (TEM) and high resolution transmission electron microscopy (HRTEM) analyses. A FESEM image is shown in Figure 4a, which indicates that the $LiFePO_4/C$ nanocomposite has huge mass loading. From the magnified FESEM image in Figure 4b, it is clearly visible that the size of

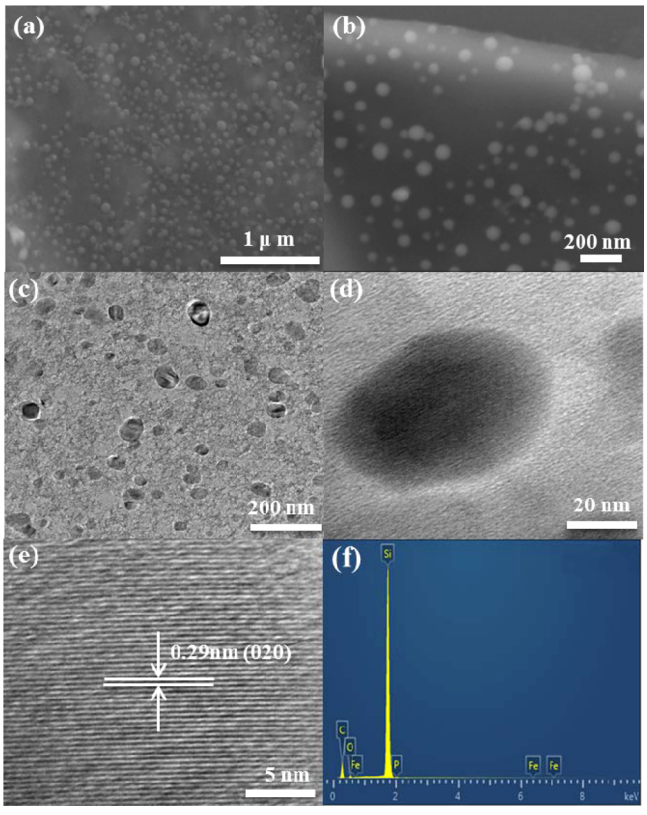

Figure 4. Typical characterizations of the $LiFePO_4/C$ nanocomposite at 750 °C. (a, b) SEM images with different magnifications. (c) Low-magnification TEM and (d) a locally enlarged TEM image to describe clearly the encapsulated $LiFePO_4$ nanoparticles. (e) HRTEM image to show the crystal structures for the encapsulated $LiFePO_4$ nanoparticles. (f) Energy-dispersive spectroscopy (EDX) of the $LiFePO_4/C$ nanocomposite.

DOI: 10.1021/acssuschemeng.5b00350
ACS Sustainable Chem. Eng. 2015, 3, 1650–1657

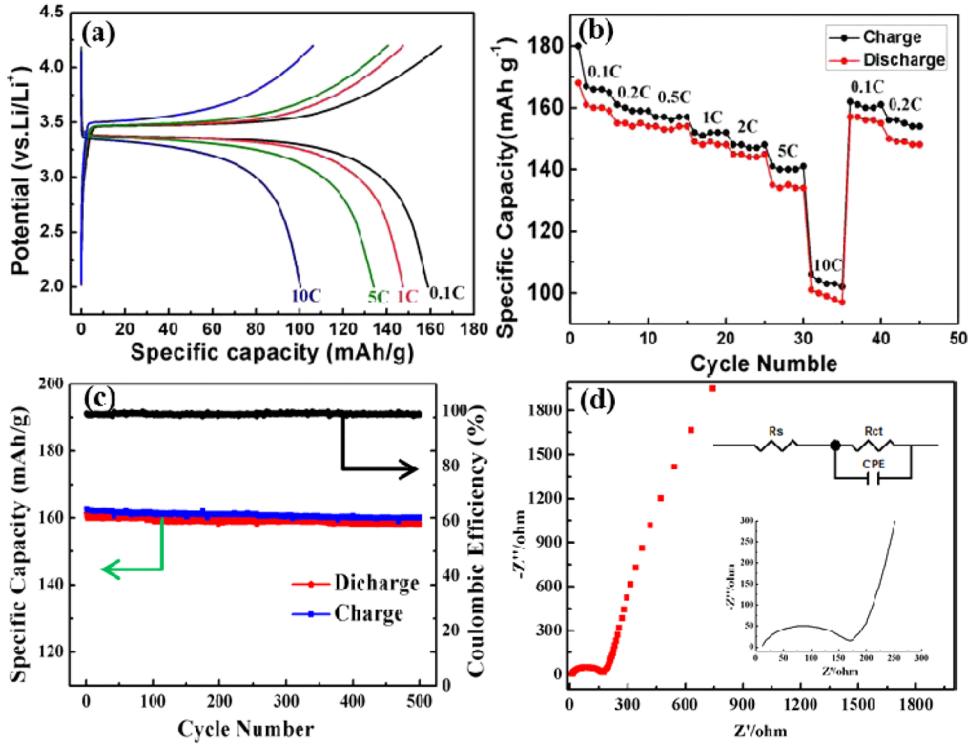

Figure 5. (a) Charge−discharge voltage profiles of the $LiFePO_4$/C at various C rates. (b) Rate-capability measurement for the $LiFePO_4$/C nanocomposite. (c) Cycling performance of the $LiFePO_4$/C nanocomposite electrode at 0.1 C. (d) AC impedance spectra of $LiFePO_4$/C nanocomposite electrode. The inset shows the magnified spectra in low frequency and the equivalent circuit.

$LiFePO_4$ nanoparticles ranges from a few nanometers to a few tens of nanometers. According to the diffusion formula $t = L^2/2D$ (where t is the diffusion time, L is the diffusion distance and D is the diffusion coefficient), reducing the particle size can significantly shorten the diffusion time of Li^+ in crystals and therefore greatly contribute to the outstanding rate capability of the $LiFePO_4$/C composite.[33] The energy-dispersive X-ray (EDX) spectroscopy analysis in Figure 4f confirms the existence of Fe, P and O in a carbon matrix. To investigate the dispersion of $LiFePO_4$ nanoparticles in the mesoporous carbon matrix, we performed TEM and HRTEM observations on the mesoporous $LiFePO_4$/C nanocomposite. Figure 4c,d presents TEM images of the $LiFePO_4$/C nanocomposite, from which it is clearly observed that $LiFePO_4$ particles are embedded in mesoporous carbon matrix. A HRTEM image (Figure 4e) taken on an individual nanoparticle exhibits clear crystal lattices with d-spacing of 0.29 nm, corresponding to the (020) plane of orthorhombic $LiFePO_4$ crystals.[36] Furthermore, the elemental distribution spectroscopy mapping of $LiFePO_4$/C nanocomposite in Figure S2 of the Supporting Information indicates that O, P and Fe are selectively distributed in the same way, matching very well with the distribution of the nanoparticles, and, however, C is fully and evenly distributed in the carbon matrix. Hence, based on FESEM and TEM characterizations, we can conclude that $LiFePO_4$/C nanocomposite has a nanosheetlike architecture, in which $LiFePO_4$ nanoparticles are randomly dotted in the mesoporous carbon framework. Theoretically, the microstructure ensures facile infiltration of electrolyte into the mesopores in Li storage, high electronic conductivity, accelerated mass transfer and rapid charge transfer.

To understand the superior electrochemical performance of the $LiFePO_4$/C nanocomposites, it is necessary to precisely study the charge−discharge curve, cyclic voltammetry (CV) and electrochemical impedance spectroscopy (EIS) profiles. Figure 5a shows the charge/discharge profiles of mesoporous $LiFePO_4$/C cathode at different current rates upon stabilization. The nanocomposite electrode delivers a discharge capacity of 159 mAh g^{-1} at 0.1 C (1 C is equal to 170 mA g^{-1}), which is very close to the theoretical capacity of $LiFePO_4$ (170 mAh g^{-1}). Although the specific capacity gradually decreases with the increasing of the current rates, a high reversible capacity of 148 mAh g^{-1} has still been achieved at 1 C. Even at the ultrahigh current rate of 10 C, a capacity of 101 mAh g^{-1} is also obtained, demonstrating that the as-prepared mesoporous $LiFePO_4$/C nanocomposite is capable of enduring high current densities' impact in charge and discharge. The rate performance of mesoporous $LiFePO_4$/C nanocomposites is demonstrated in Figure 5b and the nanocomposite electrode is subsequently tested at the varied current rates: 0.1, 0.2, 0.5, 1, 2, 5 and 10 C. It should be noted that as long as the current rate returns to the low current density, the specific capacity can be nearly recovered to the original value, manifesting that the structural integrity of the $LiFePO_4$/C cathode material has well been maintained even after longtime high-rate charge and discharge processes. The excellent rate capability is attributed to both the small size of $LiFePO_4$ nanoparticles and porous structure of the carbon matrixes, which is a desirable merit required for high power application. To test the cycle life of the mesoporous $LiFePO_4$/C nanocomposite, long-term charge/discharge cycling at 0.1 C was conducted, and the results are shown in Figure 5c, in which the charge and discharge capacity curves are almost overlapping due to the ultrahigh Coulombic efficiency of almost 99.2%. After 100 cycles, the tested cell still delivers a capacity of nearly 160 mAh g^{-1} (equal to 94.12% capacity retention), demonstrating outstanding cyclability at a low

DOI: 10.1021/acssuschemeng.5b00350
ACS Sustainable Chem. Eng. 2015, 3, 1650−1657

current rate due to the active materials' good monodispersity and great conductive networks constructed by the carbon matrixes. The electrochemical performance of the $LiFePO_4$/C nanocomposite is comparable or even better than those of previously reported $LiFePO_4$ nanoparticles embedded in nanoporous carbon matrix,[21] nanostructured $LiFePO_4$,[37] and carbon-nanotube-decorated nano-$LiFePO_4$/C composites.[38] Figure S3 of the Supporting Information shows CV curves of the $LiFePO_4$/C nanocomposite electrode at the scanning rate of 0.1 mV/s. The redox peaks in the range of 3.2−3.70 V should be attributed to the Fe^{2+} /Fe^{3+} redox couple reactions, corresponding to lithium extraction (cathodic) and insertion (anodic) from/into $LiFePO_4$ crystal structure. For comprehensive study of the electrochemical performance, AC impedance measurements are carried out and the results shown in Figure 5d. According to the Nyquist plots of the sample, the charge-transfer resistance (Rct) of $LiFePO_4$/C nanocomposite is 144.8 Ω and the Li ion diffusion resistance (Rs) is 17.88 Ω. The electrochemical impedance spectroscopy (EIS) result demonstrates that liquid electrolyte can easily flood into the carbon matrixes, ensuring the electrolyte's enhanced diffusing kinetics. For comparison, rice husks were adopted as the carbon source and $LiFePO_4$/C nanocomposite was obtained in the same way. As shown in Figure S8 of the Supporting Information, the electrochemical performance of $LiFePO_4$/C obtained via rice husk is notably inferior to that obtained via corn stalk considering the capacity, Coulombic efficiency and cycling ability.

To enrich further and widen the applicable scope of the fabrication strategy, Li_2FeSiO_4/C nanocomposite was prepared nearly in the same way. Figure 6 shows the XRD pattern of

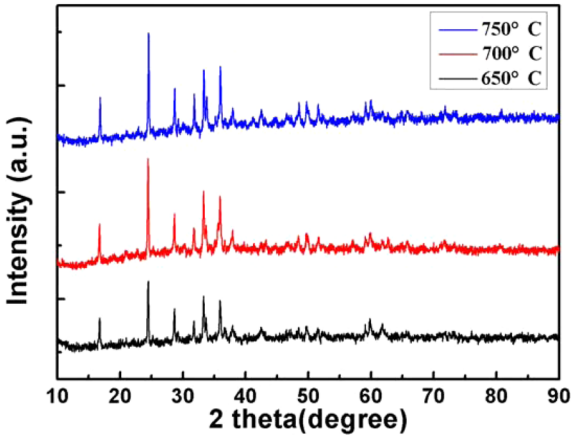

Figure 6. XRD patterns of Li_2FeSiO_4/C nanocomposite calcinated at different temperatures.

Li_2FeSiO_4/C nanocomposite calcinated at different temperatures, in which all the diffraction lines are in good agreement with the orthorhombic Li_2FeSiO_4 phase. The morphology of as-synthesized Li_2FeSiO_4/C was characterized by FESEM, as is shown in Figure 7. As shown in Figure 7a, the sheetlike carbon network is nanoporous and Li_2FeSiO_4 particles are anchored in the nanostructure. From the magnified FESEM image in Figure 7b, we can find that Li_2FeSiO_4 particles of about 20−100 nm in diameter are embedded in a nanoporous carbon matrix. The EDX mapping of Li_2FeSiO_4/C nanocomposite in Figure 7d further confirms the conclusion. The TEM image in Figure 7c demonstrates that the active nanoparticles are tightly confined

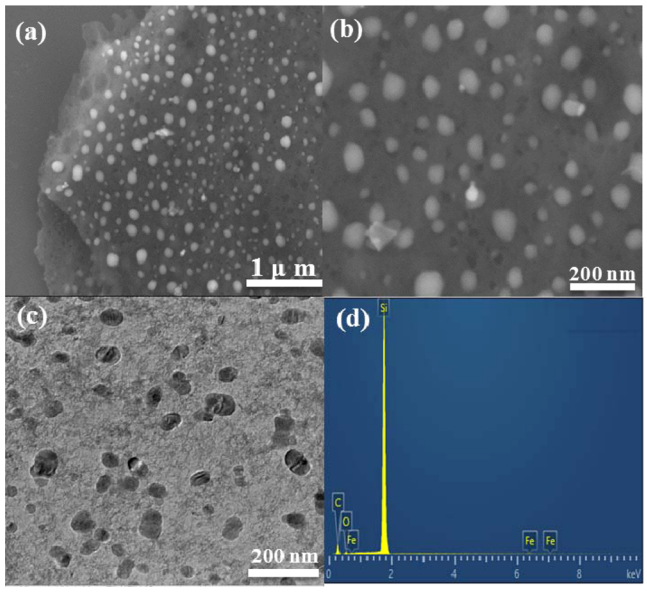

Figure 7. Typical characterizations of the Li_2FeSiO_4/C nanocomposite at 700 °C. (a, b) SEM images with different magnifications. (c) Low-magnification TEM. (d) Energy-dispersive spectroscopy (EDS) of the Li_2FeSiO_4/C nanocomposite.

in the nanoporous carbon network, preventing the nanoparticles from aggregation and pulverization. To understand the superior electrochemical performance of the Li_2FeSiO_4/C nanocomposite, we need to study clearly the charge−discharge curves. Figure 8a shows the charge/discharge profiles of mesoporous Li_2FeSiO_4/C cathodes at different current rates. The composite can deliver a discharge capacity of around 240 mAh g^{-1} at 0.1 C, reaching about 73% of the theoretical capacity of Li_2FeSiO_4. Even at the high current rate of 2 C, a capacity of 152 mAh g^{-1} is still obtained. Figure 8b demonstrates the rate capability at varied current rates: 0.1, 0.2, 0.5 and 1 C. As long as the current rate reverses to low current rate, the cell capacity can nearly recover to the original value, manifesting the outstanding rate capability of Li_2FeSiO_4/C nanocomposite. Figure S4 of the Supporting Information shows CV curves of Li_2FeSiO_4/C nanocomposite electrode at the scanning rate of 0.5 mV/s. As shown in Figure 8a, two plateaus, located around 3.2 and 2.0 V, corresponding to the successive two steps of oxidation of Fe^{2+}/Fe^{3+}/Fe^{4+}, are distinctly observed for the Li_2FeSiO_4/C electrode.[39,40] We attribute the excellent performance of this material, for example, high capacity with more than one Li^+ recycled in Li_2FeSiO_4 and high rate capability, to the novel Li_2FeSiO_4/C structure, where nanosized Li_2FeSiO_4 particles are dotted within the porous carbon frameworks. Such a structure is favorable for high reversible capacity when charged to a high voltage of 4.8 V, fast kinetics of Li^+ insertion/extraction from nanosized particles, and fast electron transfer along the porous carbon framework.[41] According to the discussion above, it is obvious to detect that the mesoporous nanoarchitecture enables not only intimate contact between electrolyte and active nanoparticles, but also high electronic conductivity and fluent mass diffusion. What's more, nanosized particles also provide a short pathway for lithium intercalation and deintercalation.[42−44] All the features mentioned above jointly contribute to the excellent cyclability and rate capability of the carbon composites evolved from natural biomass sources.

DOI: 10.1021/acssuschemeng.5b00350
ACS Sustainable Chem. Eng. 2015, 3, 1650−1657

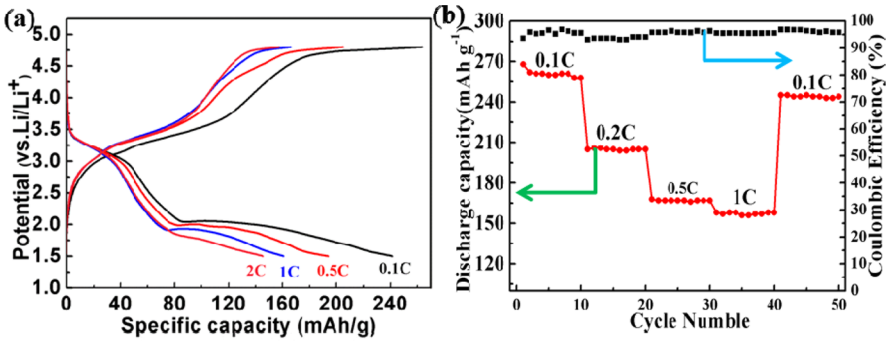

Figure 8. (a) Charge−discharge voltage profiles of the Li_2FeSiO_4/C at various C rates. (b) Rate-capability measurement for the Li_2FeSiO_4/C nanocomposite.

It should be highlighted that the method applied here is facile and universal, and has great potential to be extended to synthesis of other electrode materials for LIBs. So far, in our lab, $LiFePO_4$, Li_2FeSiO_4, $LiMnPO_4$, TiO_2, $LiFeO_2$, Sn and so on, have successfully been synthesized based on the same strategy, indicating the feasibility, extensibility and scalability for this approach. In this paper, only $LiFePO_4$ and Li_2FeSiO_4 carbon-matrixes-based nanocomposites are introduced as the examples to exhibit the method's advantages. For the next step, more functional carbon-based composite materials, such as Si, MnO_2, $LiMn_2O_4$ and LiCo/Ni/MnO_2 incorporated with carbon matrixes, will be extensively investigated in the near future.

CONCLUSION

In summary, in this paper, we have introduced a green and general strategy, where crop stalks, a major byproduct in corn harvest, can be used as carbon host matrixes with an ideal porous nanostructure for high performance Li ion batteries positive materials. Low-cost reagents and crop stalks are used to prepare pure-phase high performance $LiFePO_4$/C and Li_2FeSiO_4/C nanocomposites, in which the active particles are evenly distributed in the porous carbon framework. The achieved sheetlike composites show excellent cyclability, high reversible capacity and improved rate capability due to the unique structure. Moreover, considering the huge production of corn on a global scale, it is predictable that the general strategy could play an important role in commercializing the high performance electrode materials for the advanced Li ion batteries.

EXPERIMENTAL SECTION

Preparation of Porous $LiFePO_4$/C Nanosheet. The $LiFePO_4$/C nanosheets were prepared by solid state reaction method using LiH_2PO_4 (99.9%, Aldrich), $Fe(NO_3)_3$ (98.5%, Aldrich) and raw crop stalks as the starting materials. Crop stalks were washed with deionized water and dried at 60 °C in the oven for 2 h. 5 mL of 2 M LiH_2PO_4 and 5 mL of 2 M $Fe(NO_3)_3$ were added to 0.5 g of cut crop stalks, respectively. The intermediate products were then dried at 80 °C in the oven for 8 h. Afterward, the dried samples were loaded into the tube furnace and calcined at 700 °C/750 °C/800 °C for 200 min under Ar/H_2 (v/v = 95:5) atmosphere with a ramp of 5 °C min^{-1}.

Preparation of Porous Li_2FeSiO_4/C Nanosheet. To acquire the designed composite, the stoichiometric ratio of Li:Fe:Si = 2:1:1. The crop stalks were treated as described above. 10 mL of 2 M $LiNO_3$ (99%, Aldrich) and 5 mL of 2 M $Fe(NO_3)_3$ (98.5%, Aldrich) were dropped on the cut crop stalks, respectively. 5 mL of 2 M tetraethyl orthosilicate (TEOS) ethanol solution were then added on the crop stalks, followed by drying at 80 °C in the oven for 8 h. Finally, the dried samples were calcined at 700 °C for 200 min under Ar atmosphere with a ramp of 5 °C min^{-1}.

Characterization of the Samples. Field emission scanning electron microscopy (FESEM, JEOL, JSM-7800F), transmission electron microscopy (TEM, JEOL, JEM-2100F, 200 kV), powder X-ray diffraction (XRD, BrukerD8 Advance X-ray diffractometer with Cu K a radiation), Brunauer−Emmett−Teller surface area measurement (BET, Quantachrome Autosorb-2000 surface area and pore size analyzer), inductively coupled plasma-atomic emission spectroscopy (ICP-AES, iCAP6300 Duo) and Raman Microscopy (RENISHAW Invia, UK, voltage (AC) 100−240 V, Power 150W) were applied to characterize the obtained samples.

Electrochemical Characterization. For electrochemical tests, a homogeneous mixture composed of active material, carbon black and polyvinyl difluoride (PVDF) using 1-methyl-2-pyrrolidinone (NMP) as a solvent in a weight ratio of 80:10:10 was prepared under strong magnetic stirring for at least 1 day. The slurry was then extracted and spread on to aluminum foil. Prior to cell fabrication, the electrodes were heated in a vacuum oven at 120 °C for 8 h. The assembly of the test cells was carried out in an argon-filled glovebox using Li metal as the negative electrode. The electrolyte solution of $LiFePO_4$/C was 1 M $LiPF_6$ in a 1:1 mixture of ethylene carbonate (EC) and dimethyl carbonate (DMC) and the separator was a microporous membrane (Celgard 2400). The electrolyte solution of Li_2FeSiO_4/C was 1 M $LiPF_6$ dissolved in a mixture of ethylene carbonate (EC), dimethyl carbonate (DMC) and ethylene methyl carbonate (EMC) (1:1:1 by weight) and the separator was a microporous membrane (Celgard 2400). Besides, the cathode loading was 2 mg/cm^2. The galvanostatic charge and discharge experiment of $LiFePO_4$/C was performed in the range of 2.0−4.2 V at room temperature and Li_2FeSiO_4/C was performed in the range of 1.5−4.8 V. Cyclic voltammetry (CV) and electrochemical impedance spectroscopy (EIS) measurements of the cells were made using the two-electrode system on an electrochemical working station CHI660D. For the EIS measurements, the frequency range was between 100 kHz and 10 mHz.

ASSOCIATED CONTENT

Supporting Information

Raman spectrum of the as-prepared LiFePO4/C at 750 °C, elemental distribution spectroscopy (EDS) mapping of $LiFePO_4$/C nanocomposite, cyclic voltammograms of the as-prepared $LiFePO_4$/C nanocomposite at 750 °C, cyclic voltammograms of the as-prepared Li_2FeSiO_4/C nanocomposite at 700 °C, optical pictures for original stage of core stalks and the finally achieved electrode materials ($LiFePO_4$/C), SEM image of the synthesized Sn/C nanocomposite and the corresponding XRD profile, SEM images of the crop stalks and charge−discharge voltage profiles of the $LiFePO_4$/C obtained via rice husk at the current rate of 0.1 C and cycling performance of the $LiFePO_4$/C nanocomposite electrode at 0.1 C. The Supporting Information is available free of charge on

DOI: 10.1021/acssuschemeng.5b00350
ACS Sustainable Chem. Eng. 2015, 3, 1650−1657

the ACS Publications website at DOI: 10.1021/acssuschemeng.5b00350.

AUTHOR INFORMATION

Corresponding Author

*Y. Wang. E-mail: wangy@cqu.edu.cn; prospectwy@gmail.com.

Notes

The authors declare no competing financial interest.

ACKNOWLEDGMENTS

This work was financially supported by the Thousand Young Talents Program of the Chinese Central Government (Grant No. 0220002102003), National Natural Science Foundation of China (NSFC, Grant No. 21373280, 21403019), the Fundamental Research Funds for the Central Universities (0301005202017), Beijing National Laboratory for Molecular Sciences (BNLMS) and Hundred Talents Program at Chongqing University (Grant No. 0903005203205).

REFERENCES

(1) Beadle, G. W. Origin of corn pollen evidence. *Science* **1981**, *213*, 890−892.

(2) Parr, M.; Grossman, J. M.; Reberg-Horton, S. C.; Brinton, C.; Crozier, C. Nitrogen delivery from legume cover crops in no-till organic corn production. *Agron J.* **2011**, *103*, 1578−1590.

(3) Li, Q.; Yang, M.; Wang, D.; Li, W.; Wu, Y.; Zhang, Y.; Xing, J.; Su, Z. Efficient conversion of crop stalk wastes into succinic acid production by actinobacillus succinogenes. *Bioresour. Technol.* **2010**, *101*, 3292−3294.

(4) Xiaodong, G. Analysis of crop stalk utilization. *Trans. Chin. Soc. Agric. Eng.* **2006**, *22*, 104−106.

(5) Shapouri, H.; Duffield, J. A.; Wang, M. The energy balance of corn ethanol revisited. *Trans. ASAE* **2003**, *46*, 959−968.

(6) Isahak, W. N. R. W.; Hisham, M. W. M.; Yarmo, M. A. Highly porous carbon materials from biomass by chemical and carbonization method: A comparison study. *J. Chem.* **2013**, *2013*, 620346−620352.

(7) Srinivas, G.; Krungleviciute, V.; Guo, Z.-X.; Yildirim, T. Exceptional CO_2 capture in a hierarchically porous carbon with simultaneous high surface area and pore volume. *Energy Environ. Sci.* **2014**, *7*, 335−342.

(8) Wickramaratne, N. P.; Xu, J.; Wang, M.; Zhu, L.; Dai, L.; Jaroniec, M. Nitrogen enriched porous carbon spheres: Attractive materials for supercapacitor electrodes and CO_2 adsorption. *Chem. Mater.* **2014**, *26*, 2820−2828.

(9) Lee, J.; Kim, J.; Hyeon, T. Recent progress in the synthesis of porous carbon materials. *Adv. Mater.* **2006**, *18*, 2073−2094.

(10) Lee, J.; Yoon, S.; Hyeon, T.; Oh, S. M.; Kim, K. B. Synthesis of a new mesoporous carbon and its application to electrochemical double-layer capacitors. *Chem. Commun.* **1999**, 2177−2178.

(11) Liu, R.; Wang, X. Q.; Zhao, X.; Feng, P. Y. Sulfonated ordered mesoporous carbon for catalytic preparation of biodiesel. *Carbon* **2008**, *46*, 1664−1669.

(12) Zhang, F.; Ma, H.; Chen, J.; Li, G. D.; Zhang, Y.; Chen, J. S. Preparation and gas storage of high surface area microporous carbon derived from biomass source cornstalks. *Bioresour. Technol.* **2008**, *99*, 4803−4808.

(13) Liu, H.-j.; Bo, S.-h.; Cui, W.-j.; Li, F.; Wang, C.-x.; Xia, Y.-y. Nano-sized cobalt oxide/mesoporous carbon sphere composites as negative electrode material for lithium-ion batteries. *Electrochim. Acta* **2008**, *53*, 6497−6503.

(14) Endo, M.; Kim, C.; Nishimura, K.; Fujino, T.; Miyashita, K. Recent development of carbon materials for Li ion batteries. *Carbon* **2000**, *38*, 183−197.

(15) Li, H.; Wang, Z.; Chen, L.; Huang, X. Research on advanced materials for Li-ion batteries. *Adv. Mater.* **2009**, *21*, 4593−4607.

(16) Wang, Y.; Bai, Y.; Li, X.; Feng, Y.; Zhang, H. A general strategy towards wncapsulation of nanoparticles in sandwiched graphene sheets and the synergic effect on energy storage. *Chem.—Eur. J.* **2013**, *19*, 3340−3347.

(17) Zhang, H.; Feng, Y.; Zhang, Y.; Fang, L.; Li, W.; Liu, Q.; Wu, K.; Wang, Y. Peapod-like composite with nickel phosphide nanoparticles encapsulated in carbon fibers as enhanced anode for Li-ion batteries. *ChemSusChem* **2014**, *7*, 2000−2006.

(18) Jung, D. S.; Ryou, M. H.; Sung, Y. J.; Park, S. B.; Choi, J. W. Recycling rice husks for high-capacity lithium battery anodes. *Proc. Natl. Acad. Sci. U. S. A.* **2013**, *110*, 12229−12234.

(19) Zhang, B.; Xiao, M.; Wang, S.; Han, D.; Song, S.; Chen, G.; Meng, Y. Novel hierarchically porous carbon materials obtained from natural biopolymer as host matrixes for lithium−sulfur battery applications. *ACS Appl. Mater. Interfaces* **2014**, *6*, 13174−13182.

(20) Zhang, F.; Wang, K. X.; Li, G. D.; Chen, J. S. Hierarchical porous carbon derived from rice straw for lithium ion batteries with high-rate performance. *Electrochem. Commun.* **2009**, *11*, 130−133.

(21) Liu, N. A.; Huo, K. F.; McDowell, M. T.; Zhao, J.; Cui, Y. Rice husks as a sustainable source of nanostructured silicon for high performance Li-ion battery anodes. *Sci. Rep.* **2013**, *3*, 1919−1926.

(22) Jiang, J.; Zhu, J. H.; Ai, W.; Fan, Z. X.; Shen, X. N.; Zou, C. J.; Liu, J. P.; Zhang, H.; Yu, T. Evolution of disposable bamboo chopsticks into uniform carbon fibers: A smart strategy to fabricate sustainable anodes for Li-ion batteries. *Energy Environ. Sci.* **2014**, *7*, 2670−2679.

(23) Wang, L. P.; Schnepp, Z.; Titirici, M. M. Rice husk-derived carbon anodes for lithium ion batteries. *J. Mater. Chem. A* **2013**, *1*, 5269−5273.

(24) Wang, L. P.; Xue, J.; Gao, B.; Gao, P.; Mou, C. X.; Li, J. Z. Rice husk derived carbon-silica composites as anodes for lithium ion batteries. *RSC. Adv.* **2014**, *4*, 64744−64746.

(25) Titirici, M. M.; White, R. J.; Brun, N.; Budarin, V. L.; Su, D. S.; del Monte, F.; Clark, J. H.; MacLachlan, M. J. Sustainable carbon materials. *Chem. Soc. Rev.* **2015**, *44*, 250−290.

(26) Wei, L.; Yushin, G. Nanostructured activated carbons from natural precursors for electrical double layer capacitors. *Nano. Energy* **2012**, *1*, 552−565.

(27) Jain, A.; Aravindan, V.; Jayaraman, S.; Kumar, P. S.; Balasubramanian, R.; Ramakrishna, S.; Madhavi, S.; Srinivasan, M. P. Activated carbons derived from coconut shells as high energy density cathode material for Li-ion capacitors. *Sci. Rep.* **2013**, *3*, 3002−3008.

(28) Wu, X. L.; Chen, L. L.; Xin, S.; Yin, Y. X.; Guo, Y. G.; Kong, Q. S.; Xia, Y. Z. Preparation and Li storage properties of hierarchical porous carbon fibers derived from alginic acid. *ChemSusChem* **2010**, *3*, 703−707.

(29) Dutta, S.; Bhaumik, A.; Wu, K. C. W. Hierarchically porous carbon derived from polymers and biomass: Effect of interconnected pores on energy applications. *Energy Environ. Sci.* **2014**, *7*, 3574−3592.

(30) Wu, X. L.; Jiang, L. Y.; Cao, F. F.; Guo, Y. G.; Wan, L. J. $LiFePO_4$ Nanoparticles embedded in a nanoporous carbon matrix: Superior cathode material for electrochemical energy-storage devices. *Adv. Mater.* **2009**, *21*, 2710−2714.

(31) Takahashi, M.; Tobishima, S.; Takei, K.; Sakurai, Y. Characterization of $LiFePO_4$ as the cathode material for rechargeable lithium batteries. *J. Power Sources* **2001**, *97*−*98*, 508−511.

(32) Wang, L.; Liang, G. C.; Ou, X. Q.; Zhi, X. K.; Zhang, J. P.; Cui, J. Y. Effect of synthesis temperature on the properties of $LiFePO_4$/C composites prepared by carbothermal reduction. *J. Power Sources* **2009**, *189*, 423−428.

(33) Saravanan, K.; Balaya, P.; Reddy, M. V.; Chowdari, B. V. R.; Vittal, J. J. Morphology controlled synthesis of $LiFePO_4$/C nanoplates for Li-ion batteries. *Energy Environ. Sci.* **2010**, *3*, 457−464.

(34) Kayiran, S. B.; Lamari, F. D.; Levesque, D. Adsorption properties and structural characterization of activated carbons and nanocarbons. *J. Phys. Chem. B* **2004**, *108*, 15211−15215.

(35) Bruce, P. G.; Scrosati, B.; Tarascon, J. M. Nanomaterials for rechargeable lithium batteries. *Angew. Chem., Int. Ed.* **2008**, *47*, 2930−2946.

(36) Ellis, B.; Kan, W. H.; Makahnouk, W. R. M.; Nazar, L. F. Synthesis of nanocrystals and morphology control of hydrothermally prepared $LiFePO_4$. *J. Mater. Chem.* **2007**, *17*, 3248−3254.
(37) Prosini, P. P.; Carewska, M.; Scaccia, S.; Wisniewski, P.; Pasquali, M. Long-term cyclability of nanostructured $LiFePO_4$. *Electrochim. Acta* **2003**, *48*, 4205−4211.
(38) Wu, X. L.; Guo, Y. G.; Su, J.; Xiong, J. W.; Zhang, Y. L.; Wan, L. J. Carbon-nanotube-decorated nano-$LiFePO_4$@C cathode material with superior high-rate and low-temperature performances for lithium-ion batteries. *Adv. Energy Mater.* **2013**, *3*, 1155−1160.
(39) Muraliganth, T.; Stroukoff, K. R.; Manthiram, A. Microwave-solvothermal synthesis of nanostructured Li_2MSiO_4/C (M = Mn and Fe) cathodes for lithium-ion batteries. *Chem. Mater.* **2010**, *22*, 5754−5761.
(40) Lv, D. P.; Wen, W.; Huang, X. K.; Bai, J. Y.; Mi, J. X.; Wu, S. Q.; Yang, Y. A novel Li_2FeSiO_4/C composite: Synthesis, characterization and high storage capacity. *J. Mater. Chem.* **2011**, *21*, 9506−9512.
(41) Bai, J.; Gong, Z.; Lv, D.; Li, Y.; Zou, H.; Yang, Y. Nanostructured $0.8Li_2FeSiO_4/0.4Li_2SiO_3$/C composite cathode material with enhanced electrochemical performance for lithium-ion batteries. *J. Mater. Chem.* **2012**, *22*, 12128−12132.
(42) Oh, S. W.; Myung, S. T.; Oh, S. M.; Oh, K. H.; Amine, K.; Scrosati, B.; Sun, Y. K. Double carbon coating of $LiFePO_4$ as high rate electrode for rechargeable lithium batteries. *Adv. Mater.* **2010**, *22*, 4842−4845.
(43) Vu, A.; Stein, A. Multiconstituent synthesis of $LiFePO_4$/C composites with hierarchical porosity as cathode materials for lithium ion batteries. *Chem. Mater.* **2011**, *23*, 3237−3245.
(44) Lou, X. W.; Deng, D.; Lee, J. Y.; Archer, L. A. Thermal formation of mesoporous single-crystal Co_3O_4 nano-needles and their lithium storage properties. *J. Mater. Chem.* **2008**, *18*, 4397−4401.

DOI: 10.1021/acssuschemeng.5b00350
ACS Sustainable Chem. Eng. 2015, 3, 1650−1657